Supporting Information

Cationic π-Conjugated Polyelectrolyte Shows Antimicrobial Activity by Causing Lipid Loss and Lowering Elastic Modulus of Bacteria

Ehsan Zamani,[1,†] Tyler J. Johnson,[1,†] Shyambo Chatterjee,[1] Cheryl Immethun,[1] Anandakumar Sarella,[2] Rajib Saha,[1] Shudipto Konika Dishari[1,*]

[1,] Department of Chemical and Biomolecular Engineering, University of Nebraska-Lincoln, Lincoln, Nebraska 68588, United States*

[2] Nebraska Center for Materials and Nanoscience, Voelte-Keegan Nanoscience Research Center, University of Nebraska-Lincoln, Lincoln, NE 68588-0298, United States

[†] E.Z. and T.J.J. contributed equally in this work.

*Corresponding author's email: sdishari2@unl.edu; Phone: 402-472-7537.

KEYWORDS: *Antimicrobial, cationic conjugated polyelectrolytes, antibiotic-resistant, outer membrane, elastic modulus, lipid loss.*

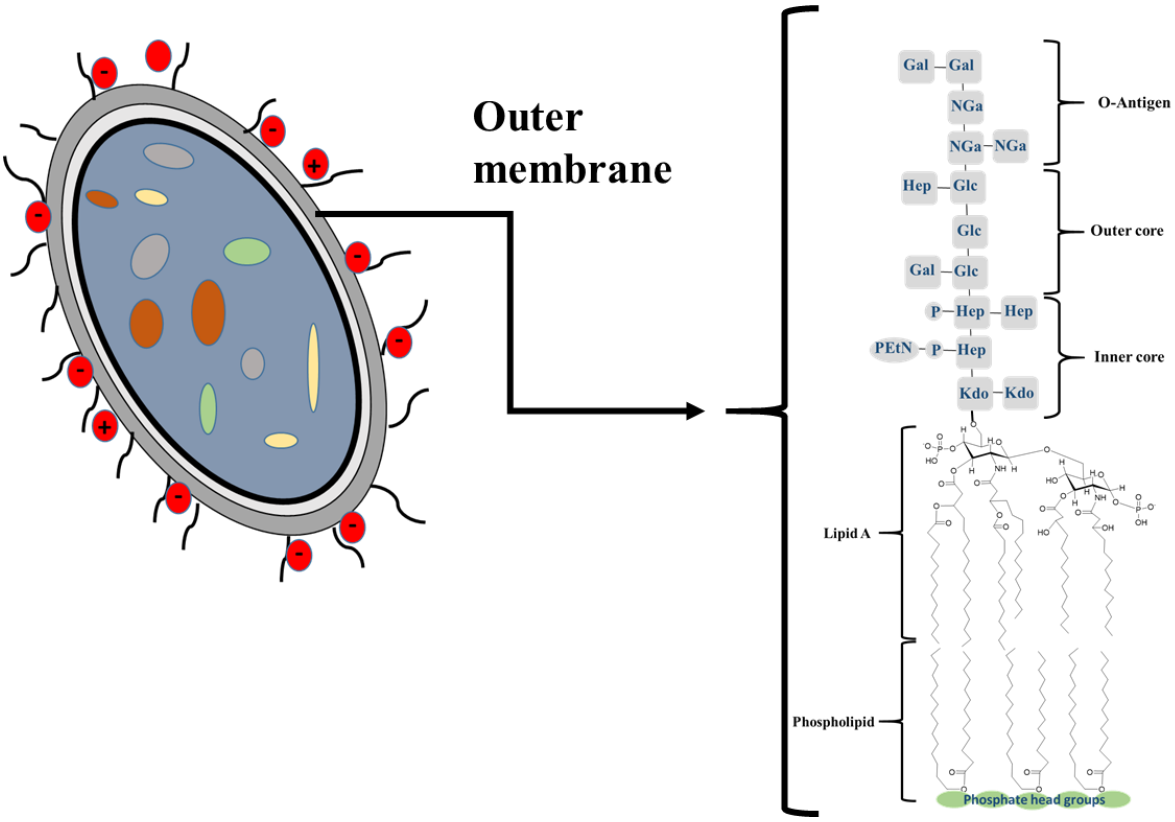

Figure S1. Schematic representation of the outer membrane of the *E. coli* cells and major components of the outer membrane (NGc: Glucosamine; NGa: Galactosamine; Glc: D-glucose; Gal: D-Galactose; Hep: L-glycero-D-manno-heptose; Kdo: 3-deoxy-D-oct-2-ulosonic acid; p: phosphate; PEtN: phosphoethanolamine).

AFM force and elastic modulus measurement.

For the cantilevers used in force curve measurements (model TR400PB, Olympus Microcantilevers, Tokyo, Japan) the cantilever spring constant (k) was determined as 33.5 ± 0.8 pN/nm (n=5) using the thermal resonance method.[1] The inverse optical laser sensitivity (invOLS; units of nm/V) was then determined automatically by the software using the noncontact method,[2] and with the known cantilever spring constant from the thermal calibration. Knowledge of the

invOLS is necessary to convert the cantilever deflection voltage (obtained from the laser incident on the photodiode detector) to a measure of vertical deflection of cantilever (d). Multiplying deflection voltage by invOLS gave the values of d. Hence, the force on the cantilever beam can be determined by Hooke's law, $F = kd$. Force curves were performed on the untreated and P1-treated cells at a piezo rate of ~ 720 nm/s until the maximum deflection of cantilever ~ 50 nm was attained, which is equivalent to ~ 1.5 nN of force (maximum) for the cantilevers used. The cantilever deflection was fixed to gain control over the indentation depth; i.e. depth the cantilever tip penetrates into the sample to create an "indent." Because it was desired to probe the mechanical properties of the bacterial cell wall in particular, the indentation depth was kept small enough to primarily investigate the cell wall, but high enough such that sufficient data could be collected for fitting purposes.[3] For a fixed deflection of cantilever, the displacement of the sample stage in z-direction was measured which gave us the value of indentation depth. In a typical force vs displacement curve (like in Figure S2), the term "displacement" actually means this "indentation depth."

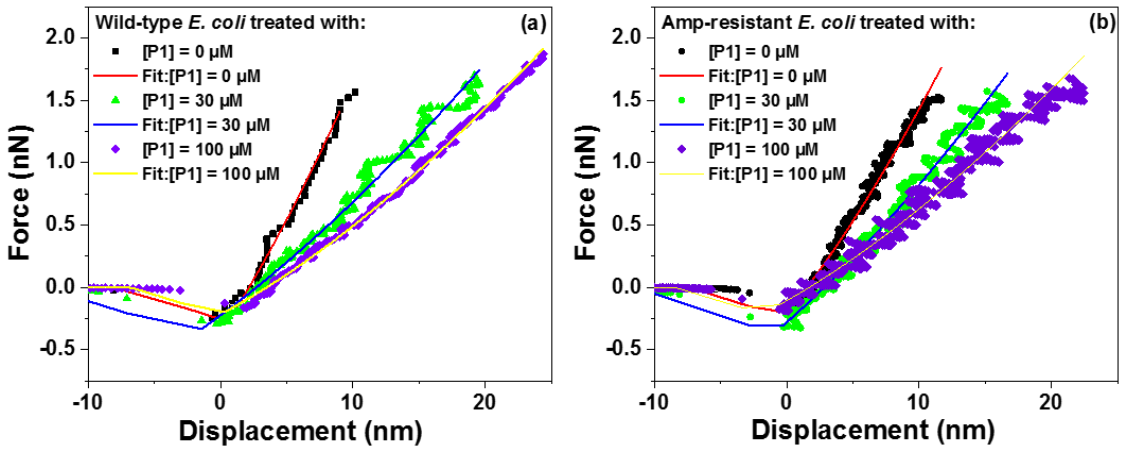

Figure S2. Typical force-displacement curve and fitting curves for untreated and P1 treated wild-type (a), and amp-resistant (b) *E. coli* cells.

Due to the presence of the jump-to-contact phenomena observed in the force-displacement curves of our indentation measurements, an adhesive contact mechanics model was required for fitting.[4] The adhesive contact mechanics models which were available to use in Igor Pro 15 software suite were the Johnson-Kendall-Roberts (JKR) model and the Derjaguin-Muller-Toprov

(DMT) model.[4,5] In general, the JKR model is best suited for larger cantilever radii on soft samples, while the DMT model is better for sharp cantilevers on hard materials. To be sure, the Tabor parameter $\mu=(R\gamma^2/E^2\varepsilon^3)^{1/3}$ was used to choose the most appropriate model.[4,5] Here, R is the radius of the spherical cantilever tip (taken as 30 nm by the manufacturer specifications), γ is the work of adhesion (surface energy per unit surface area), E is the Young's modulus of the cell, and ε is the equilibrium separation distance (typically 0.3 – 0.5 nm). The guidelines for choosing the appropriate model are such that $\mu < 0.1$ for DMT and $\mu > 5$ for JKR.[5,6] In our work, we observed $\mu \approx 100$ for measurements on both untreated and treated bacteria specimens, so the JKR model was selected. The fitting of the force curves was performed automatically via the Igor Pro 15 software suite. The fitting algorithm was supplied with an initial guess of the Young's modulus of the sample, as well as values for force and indentation depth offset to determine the point of initial contact (i.e. the point before which the jump-to-contact phenomena is prevalent)[7,8] for fitting purposes. The guess for the Young's modulus of the sample was set to 2 MPa. The guesses for force and depth offset were usually supplied automatically by the software suite. A detailed analysis of the force-displacement curve fitting for AFM indentation measurements is given by following the literatures.[7,8]

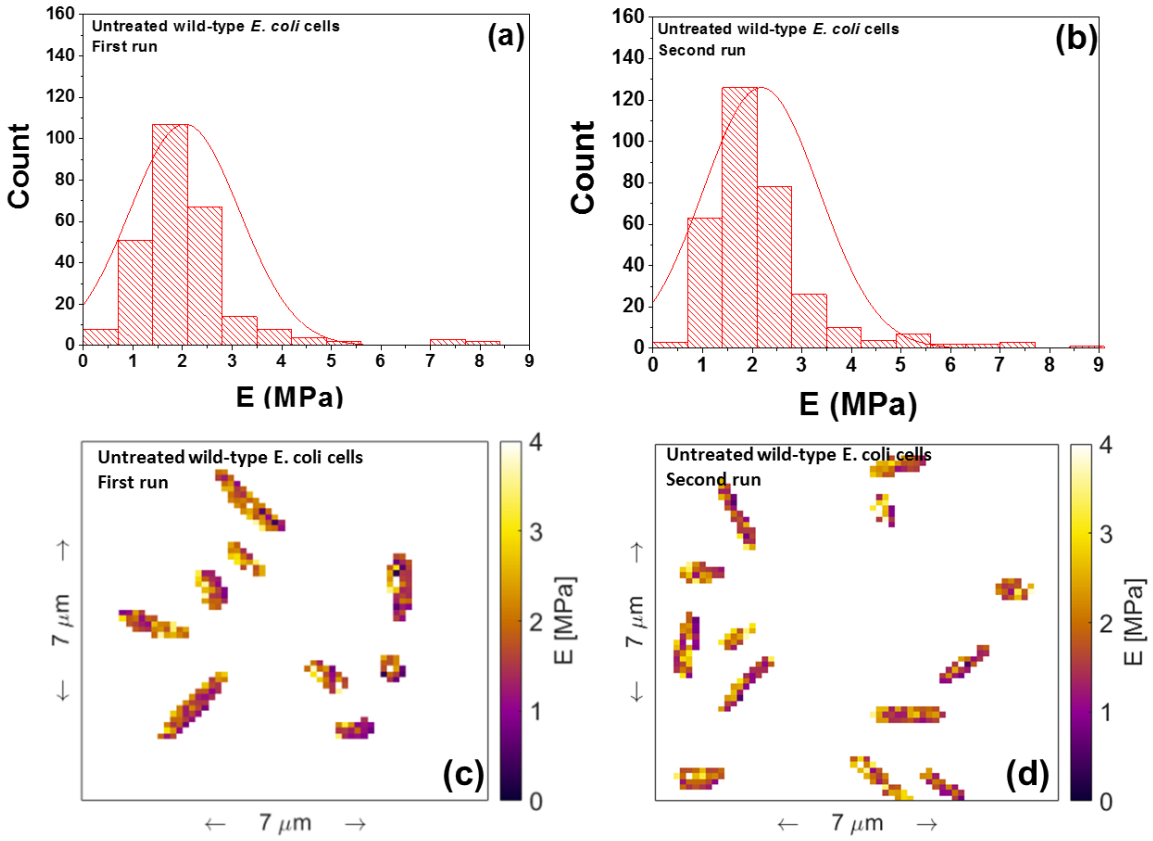

Figure S3. Histograms (with Gaussian distributions (red lines)) of Young's modulus (a, b) and force maps (c, d) of untreated wild-type *E. coli* cells. P-value for two data sets of untreated wild-type *E. coli* was more than 0.05, indicating repeatability of the results.

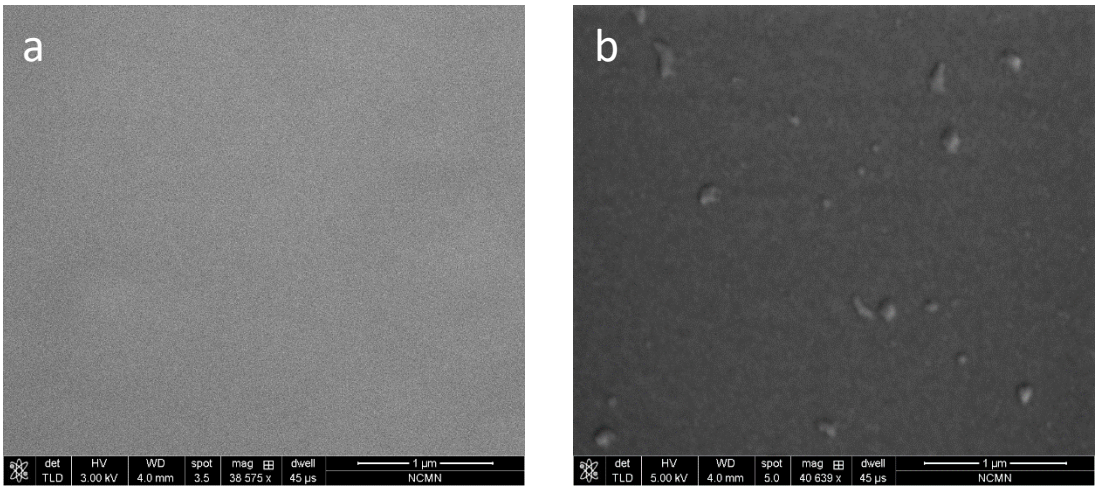

Figure S4. SEM images of the supernatant samples separated from untreated (a) and treated (b) amp-resistant *E. coli* cells.

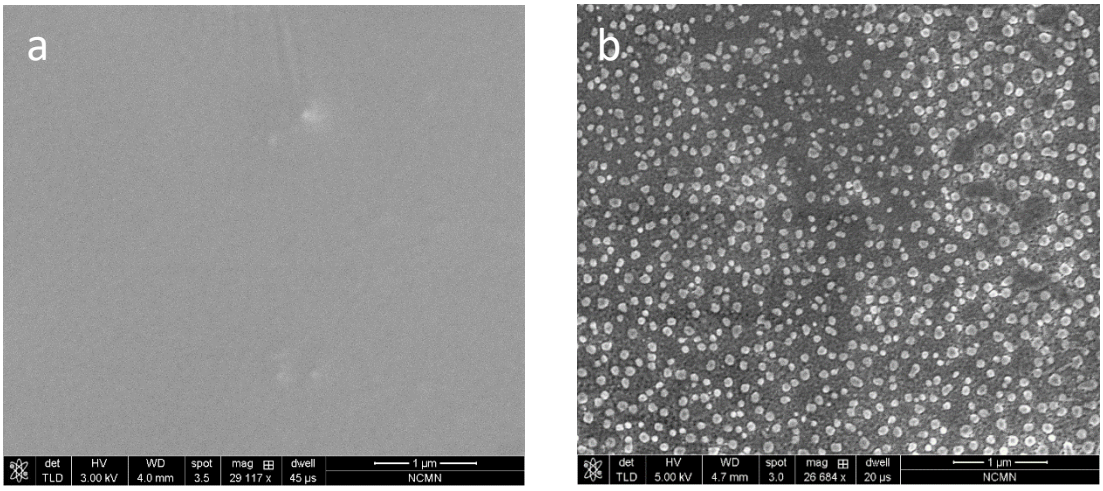

Figure S5. SEM images of filtered vesicles collected from untreated (a) and treated (b) amp-resistant *E. coli* samples.

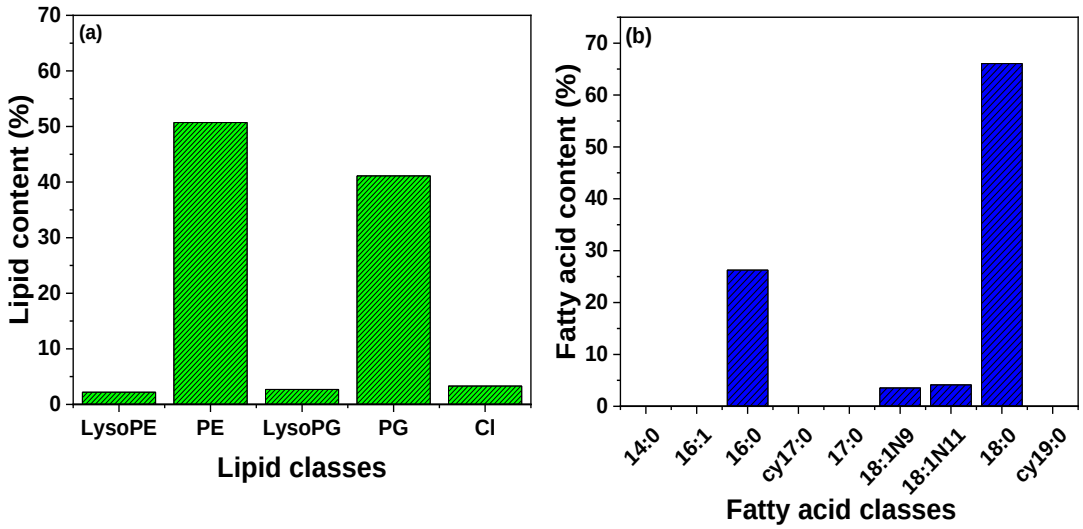

Figure S6. Lipid (a) and fatty acid (b) contents (%) in vesicles separated from treated amp-resistant *E. coli* cells.

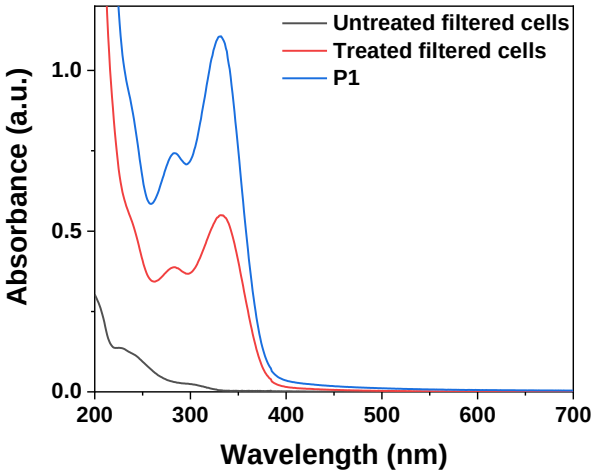

Figure S7. UV-Vis absorbance of vesicle samples filtered from untreated and treated amp-resistant *E. coli* cells and P1.

References

(1) Hutter, J. L.; Bechhoefer, J. Calibration of Atomic-Force Microscope Tips. *Rev. Sci. Instrum.* **1993**, *64*, 1868–1873.

(2) Prokschj, M. J. H.; Polcik, E. S.; Endooj, S. M.; Jarvis, P. C. P. Noninvasive Determination of Optical Lever Sensitivity in Atomic Force Microscopy. *Rev. Sci. Instrum.* **2006**, *77*, 1–5.

(3) Touhami, A.; Nysten, B.; Dufrêne, Y. F. Nanoscale Mapping of the Elasticity of Microbial Cells by Atomic Force Microscopy. *Langmuir.* **2003**, *19*, 4539–4543.

(4) Johnson, K. L.; Kendall, K.; Roberts, A. D. Surface Energy and the Contact of Elastic Solids. *Proc. R. Soc. A Math. Phys. Eng. Sci.* **1971**, *324*, 301–313.

(5) Grierson, D. S.; Flater, E. E.; Carpick, R. W. Accounting for the JKR – DMT Transition in Adhesion and Friction Measurements with Atomic Force Microscopy. *J. Adhes. Sci. Technol.* **2012**, *19*, 291–311.

(6) Song, Z.; Komvopoulos, K. Adhesion-Induced Instabilities in Elastic and Elasticplastic Contacts during Single and Repetitive Normal Loading. *J. Mech. Phys. Solids* **2011**, *59*, 884–897.

(7) Lin, D. C.; Dimitriadis, E. K.; Horkay, F. Robust Strategies for Automated AFM Force Curve Analysis - I. Non-Adhesive Indentation of Soft, Inhomogeneous Materials. *J. Biomech. Eng.* **2007**, *129*, 430–440.

(8) Lin, D. C.; Dimitriadis, E. K.; Horkay, F. Robust Strategies for Automated AFM Force Curve Analysis - II: Adhesion-Influenced Indentation of Soft, Elastic Materials. *J. Biomech. Eng.* **2007**, *129*, 904–912.